Anal. Chem. **2005,** *77,* 3651−3659

Depth Profiling of Peptide Films with TOF-SIMS and a C_{60} Probe

Juan Cheng and Nicholas Winograd*

Department of Chemistry, The Pennsylvania State University, 104 Chemistry Building, University Park, Pennsylvania 16802

A buckminsterfullerene ion source is employed to characterize peptide-doped trehalose thin films. The experiments are designed to utilize the unique sputtering properties of cluster ion beams for molecular depth profiling. The results show that trehalose films with high uniformity can be prepared on Si by a spin-coating technique. Bombardment of the film with C_{60}^+ results in high quality time-of-flight secondary ion mass spectrometry spectra, even during ion doses of up to 3×10^{14} ions/cm^2. This result is in contrast to atomic bombardment experiments in which the dose of incident ions must be kept below 10^{12} ions/cm^2 so as to retain mass spectral information. Moreover, since the films are of uniform thickness, it is possible to depth-profile through the film and into the Si substrate. This experimental protocol allows the yield of trehalose molecular equivalents and the degree of interface mixing to be evaluated in detail. When doped with a variety of small peptides up to a molecular weight of *m/z* 500, we find that the peptide molecular ion intensity remains stable under continuous C_{60}^+ bombardment, although some decrease in intensity is observed. The results are interpreted in terms of a model whereby the high trehalose yield and low damage depth of the C_{60} projectile combine to prevent damage accumulation. In general, the peptide−trehalose system provides a valuable model for evaluating the parameters that lead to effective 3-dimensional characterization of biomaterials.

Time-of-flight secondary ion mass spectrometry (TOF-SIMS) is a unique tool for characterizing molecular surfaces with high lateral resolution.[1] With this method, a focused beam of energetic ions is utilized to desorb the target molecules from a known spot on the sample. Since spectra are accumulated at the rate of up to 10 000/s,[2] it is feasible to acquire enough spectra to form an image with lateral resolution on the order of 100 nm by rastering the beam over the sample.[1] An important application of this technology is in imaging of biomaterials, particularly tissue samples[3,4] and single biological cells.[5−7] The goal is to map the chemical composition of small molecules within these materials.

There are two major difficulties that prevent development of this tool to its full capability. First, the ion beam induces significant fragmentation of molecules during desorption, which increases the congestion of the mass spectra and destroys the chemical nature of the sample itself. This latter effect is particularly noticeable if the dose of primary ions exceeds ∼1% of the number of surface molecules.[8] This result is in contrast to MALDI mass spectrometry, in which mainly unfragmented molecular ions are desorbed by the laser pulse. Second, and partly because of the dose restrictions, the number of molecules available for analysis becomes vanishingly small as the pixel size approaches 0. For example, if there are 1 000 000 molecules per square micrometer and 1% of these are sputtered, then with an ionization efficiency of <1 part in 10^4, only 1 molecule would be available for detection. It is easy to see why the signal is small.

Among the many efforts devoted to enhancing the secondary ion intensity, an essential indicator of the sensitivity, is the use of polyatomic primary projectiles. Experiments with these types of ion beams have shown significant signal enhancement, as compared to traditional atomic primary ion projectiles, especially for organic compounds with masses between 500 and 5000 Da.[9] Projectiles under development include SF_5^+, Au_3^+, Bi_3^+, and C_{60}^+. Although the reasons behind the signal enhancements are not completely understood, it is known that the kinetic energy of the individual atoms in the cluster is lower than the corresponding atomic projectile and will, hence, deposit energy closer to the target surface. The fact that multiple collision cascades are initiated simultaneously may also contribute to nonlinear enhancement effects.[10−12]

Perhaps the most intriguing property of cluster bombardment involves the fact that in some cases, chemical damage does not

* Corresponding author. Phone: 814-863-0001. Fax: 814-863-0618. E-mail: nxw@psu.edu.

(1) Pacholski, M. L.; Winograd, N. *Chem. Rev.* **1999**, *99*, 2977−3005.
(2) Braun, R. M.; Beyder, A.; Xu, J. Y.; Wood, M. C.; Ewing, A. G.; Winograd, N. *Anal. Chem.* **1999**, *71*, 3318−3324.
(3) Touboul, D.; Halgand, F.; Brunelle, A.; Kersting, R.; Tallarek, E.; Hagenhoff, B.; Laprevote, O. *Anal. Chem.* **2004**, *76*, 1550−1559.
(4) Sjoevall, P.; Lausmaa, J.; Johansson, B. *Anal. Chem.* **2004**, *76*, 4271−4278.
(5) Colliver, T. L.; Brummel, C. L.; Pacholski, M. L.; Swanek, F. D.; Ewing, A. G.; Winograd, N. *Anal. Chem.* **1997**, *69*, 2225−2231.
(6) Ostrowski, S. G.; Van Bell, C. T.; Winograd, N.; Ewing, A. G. *Science (Washington, DC)* **2004**, *305*, 71−74.
(7) Cliff, B.; Lockyer, N.; Jungnickel, H.; Stephens, G.; Vickerman, J. C. *Rapid Commun. Mass Spectrom.* **2003**, *17*, 2163−2167.
(8) Benninghoven, A.; Jaspers, D.; Sichtermann, W. *Appl. Phys. (Berlin)* **1976**, *11*, 35−39.
(9) Xu, J.; Szakal, C. W.; Martin, S. E.; Peterson, B. R.; Wucher, A.; Winograd, N. *J. Am. Chem. Soc.* **2004**, *126*, 3902−3909.
(10) Postawa, Z.; Czerwinski, B.; Szewczyk, M.; Smiley, E. J.; Winograd, N.; Garrison, B. J. *J. Phys. Chem. B* **2004**, *108*, 7831−7838.
(11) Postawa, Z.; Czerwinski, B.; Szewczyk, M.; Smiley, E. J.; Winograd, N.; Garrison, B. J. *Anal. Chem.* **2003**, *75*, 4402−4407.
(12) Colla, T. J.; Aderjan, R.; Kissel, R.; Urbassek, H. M. *Phys. Rev. B* **2000**, *62*, 8487−8493.

10.1021/ac048131w CCC: $30.25
Published on Web 04/29/2005

appear to accumulate on the sample surface. Doses in excess of the 1% restriction still allow the mass spectra to retain molecule-specific information.[13−17] In fact, there have been a few specific cases in which stable signals are observed during the removal of several hundred nanometers of material.[13,16,18,19] If these observations could be generalized, it would be feasible to perform molecular depth profiles through solid film samples. Moreover, the number of molecules in a pixel would expand from two dimensions to three dimensions. For our hypothetical pixel of 1 μm^2, for example, there are 10^9 molecules in the 1-μm cube (voxel), an easily detectable number. This idea has, of course, been utilized in atomic depth profiling of semiconductors for many years.[20] Hence, the combination of polyatomic or cluster bombardment, molecular depth profiling and mass spectral imaging would greatly expand the prospects for characterizing various biomaterials.

A key to understanding how molecules are removed from surfaces without residual damage is to be able to prepare substrates as uniform thin films. Several techniques have been examined. Vapor-phase deposition (VPD) was used by Gillen and co-workers to prepare thin films of glutamate.[13,21] This method is fast, and the films are uniform, but the molecules must be thermally stable, a problem for complex biological molecules, such as peptides and proteins. Langmuir−Blodgett (LB) technology is also a powerful approach to preparing well-defined films. These films are ordered and uniform and may consist of a single layer or many layers, up to a depth of several wavelengths of visible light.[14,22] The molecules are restricted, however, to those that have the correct hydrophilic/hydrophobic character. Finally, spin-casting is a simple approach to preparing uniform thin films. It is most often employed with polymer films in material studies, and a specific viscosity is required for the solution to be spin-cast uniformly. Because of the difficulty of preparing uniform thin films of organic materials, the number of depth profiling examples utilizing them has been limited.

Here, we show that it is possible to acquire high-quality molecular depth profiles of peptide molecules with molecular weights up to 500 Da. These profiles are possible to achieve by preparing the peptide in a solution of trehalose, followed by standard spin-coating protocols. Trehalose is a naturally occurring sugar formed by a 1,1 linkage of two D-glucose molecules. It is widespread in a variety of biological species and is a key factor in the survival of anhydrobionts in harsh dehydration environments.[23−25] In the past decade, several studies have shown that trehalose can greatly enhance the stability of biomaterials.[26−30] It was first employed in TOF-SIMS studies to preserve the conformation of adsorbed proteins.[26] With its inert nature and high solution viscosity, we find that it is straightforward to prepare thick and uniform films in a reproducible fashion. This type of platform is extremely valuable for the measurement of fundamental parameters, such as sputtering yield and damage accumulation rate. In this study, we employ a C_{60}^+ ion source to perform depth profiles through films composed of trehalose and different peptides. Molecular ions of both trehalose and the peptides were retained through the films with a sputtering yield of 300−500 molecules/impact. The study suggests that the high yield and low damage depth of the C_{60} projectile combine to prevent damage accumulation.

EXPERIMENTAL SECTION

Materials and Film Preparation. Trehalose, peptides, and solvents were purchased from Sigma-Aldrich and used without further purification. The presliced 5 mm × 5 mm Si wafer was supplied by Ted Pella Inc. (Redding, CA). The water used in preparation of all films was purified by a Milli-Q System (Millipore, Burlington, MA) and had a resistivity of 18.2 MΩ cm with an organic content of <5 ppb. To prepare a film, peptides were dissolved in water at concentrations of up to 10 mM. A 0.15-mL peptide solution was mixed with a 0.15-mL 1 M aqueous trehalose solution. The mixture was then spin-cast onto a Si wafer spinning at a speed of 3500 rpm. A uniform colored film with a glassy appearance is normally obtained. More details regarding this procedure are presented below.

Instrumentation. The TOF-SIMS instrumentation has been described in detail elsewhere[31] and is briefly discussed below. The instrument is equipped with a C_{60}^+ primary ion source, which is directed at a 40° angle relative to the surface normal. This C_{60}^+ primary ion beam system is obtained from Ionoptika Ltd (Southampton, U.K.), and a detailed characterization has been reported recently.[17] The source is operated at an anode voltage of 20 keV. At this primary ion energy, a dc beam current of >3 nA of pure C_{60}^+ can be obtained at the target by use of a 1000-μm beam-defining aperture, a 2.3-A electron beam filament current, and a 40-V grid voltage.

For depth profiling, the C_{60}^+ ion beam was operated in dc mode to sputter through the film at an area of 400 μm × 400 μm in 5 s intervals. Between erosion cycles, TOF mass spectra were taken by C_{60}^+ at an ion fluence of 10^{10} cm^{-2} into a zoomed area of 200 μm × 200 μm inside the crater. The mass spectrometer was operated in a delayed extraction mode, and a delay time of 50 ns was set between the primary ion pulse (duration 50 ns) and the secondary ion extraction pulse. Charge compensation is found to

(13) Gillen, G.; Roberson, S. *Rapid Commun. Mass Spectrom.* **1998**, *12*, 1303−1312.
(14) Sostarecz, A. G.; McQuaw, C. M.; Wucher, A.; Winograd, N. *Anal. Chem.* **2004**, *76*, 6651−6658.
(15) Wucher, A.; Sun, S.; Szakal, C.; Winograd, N. *Anal. Chem.* **2004**, *76*, 7234−7242.
(16) Szakal, C.; Sun, S.; Wucher, A.; Winograd, N. *Appl. Surf. Sci.* **2004**, *231−232*, 183−185.
(17) Weibel, D.; Wong, S.; Lockyer, N.; Blenkinsopp, P.; Hill, R.; Vickerman, J. C. *Anal. Chem.* **2003**, *75*, 1754−1764.
(18) Wagner, M. S. *Anal. Chem.* **2004**, *76*, 1264−1272.
(19) Mahoney, C. M.; Roberson, S. V.; Gillen, G. *Anal. Chem.* **2004**, *76*, 3199−3207.
(20) Hofmann, S. *Rep. Prog. Phys.* **1998**, *61*, 827−888.
(21) Gillen, G.; King, L.; Freibaum, B.; Lareau, R.; Bennett, J.; Chmara, F. *J. Vac. Sci. Technol., A* **2001**, *19*, 568−575.
(22) Blodgett, K. B. *J. Am. Chem. Soc.* **1935**, *57*, 1007−1022.
(23) Crowe, J. H.; Crowe, L. M.; Chapman, D. *Science (Washington, DC)* **1984**, *223*, 701−703.
(24) Westh, P.; Ramlov, H. *J. Exp. Zool.* **1991**, *258*, 303−311.
(25) Crowe, J. H.; Crowe, L. M. *Nat. Biotechnol.* **2000**, *18*, 145−146.
(26) Xia, N.; May, C. J.; McArthur, S. L.; Castner, D. G. *Langmuir* **2002**, *18*, 4090−4097.
(27) Guo, N.; Puhlev, I.; Brown, D. R.; Mansbridge, J.; Levine, F. *Nat. Biotechnol.* **2000**, *18*, 168−171.
(28) Singer, M. A.; Lindquist, S. *Mol. Cell* **1998**, *1*, 639−648.
(29) Roser, B. *Biopharm. Technol. Bus.* **1991**, *4*, 47−52.
(30) Xia, N.; Shumaker-Parry, J. S.; Zareie, M. H.; Campbell, C. T.; Castner, D. G. *Langmuir* **2004**, *20*, 3710−3716.
(31) Braun, R. M.; Blenkinsopp, P.; Mullock, S. J.; Corlett, C.; Willey, K. F.; Vickerman, J. C.; Winograd, N. *Rapid Commun. Mass Spectrom.* **1998**, *12*, 1246−1252.

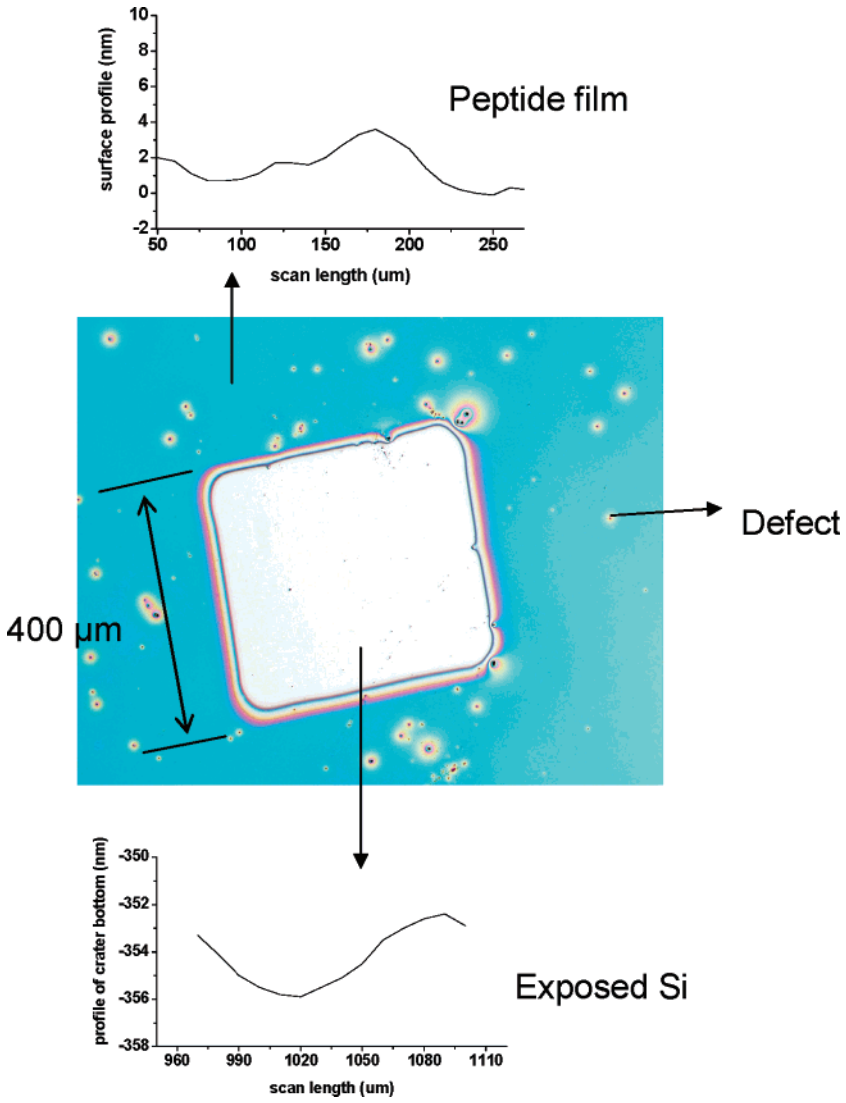

Figure 1. An optical image of the peptide film after depth profiling with C_{60}^+. In the middle is the crater and the exposed Si substrate. Surrounding is the untouched peptide film in blue-green color. Defects are also seen on the film, which are probably caused by particulates in the air when the film was spin-cast. Above and below are profiles of the film surface and the crater bottom. The roughness, estimated as twice the rms height fluctuations, typically ranges from 2 to 7 nm.

be unnecessary for the positive ion SIMS mode. The value of the signal intensity is calculated from the integrated peak area at the corresponding mass value. With these parameters, a mass resolution of ~2500 was achieved at the mass of the molecular ion for each peptide.

Profilometry. The thickness of the film is determined by a Dektak3 profilometer. After depth profiles, the silicon substrate is exposed. The profilometer is normally scanned across the crater at medium speed, and the values are averaged over five measurements.

RESULTS AND DISCUSSION

The goal of this work is to provide a highly reproducible platform for investigation of the factors that allow a stable molecular ion signal to be observed during the 3-dimensional analysis of biological materials. To establish this platform, we first describe the procedure for synthesizing uniform thin films of a trehalose glass and describe the response of this film to depth profiling by C_{60}^+ ion beams. With this structure acting as a control, we next report on depth profiles of these films after doping with small peptides of various molecular weights. Finally, these films are characterized with respect to the removal rate of sugar molecules and the propensity of the film to accumulate chemical damage.

Trehalose Film Preparation and Depth Profiling. Trehalose films are prepared by depositing 300 μL of a 0.5 M aqueous solution of trehalose in 10-μL aliquots onto the Si wafer. Each aliquot was allowed to spin for 15 s before the subsequent aliquot was applied. The wafer at room temperature is attached to a spin-coater rotating at 3500 rpm. During the deposition process, the film is visually observed to dehydrate and to form a film with a glassy character. The resulting film is confirmed to be of uniform thickness by visual inspection of the optical interference pattern that gives rise to its color. The films are generally stable to atmosphere for several hours to several days, although exposure to high humidity conditions may accelerate the conversion of the glassy film to a crystallized film that exhibits unacceptable

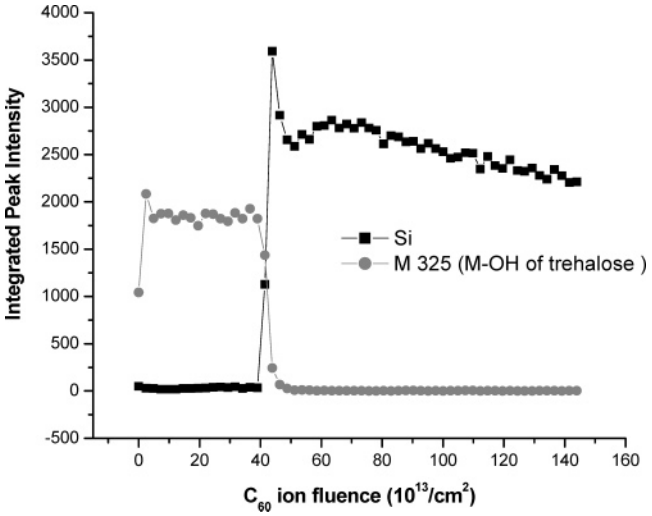

Figure 2. Depth profile of a pure trehalose film with a thickness of 780 ± 5 nm. Secondary ion intensities of trehalose at *m*/*z* 325 $(M - OH)^+$ and Si^+ at *m*/*z* 28 are plotted versus accumulated C_{60}^+ ion fluence.

topography. Using this procedure, films of a consistent thickness are produced; for this case, ~400 nm. It is possible to prepare thinner or thicker films by adjusting the concentration of the aqueous trehalose solution. For example, a 1.0 M trehalose solution yields a film of thickness of ~1000 nm.

Depth profiling of these samples is carried out using the C_{60}^+ primary ion beam both to sputter through the film and to collect mass spectra between sputtering cycles. During each cycle, the surface is irradiated with the C_{60}^+ beam for 5 s into a 400 μm × 400 μm area. To avoid edge effects associated with the formation of the crater and the finite diameter of the C_{60}^+ probe beam of ~50 μm, SIMS spectra are acquired from a 200 μm × 200 μm area in the center of the sputtered area. The sequence is controlled by computer in order to ensure accuracy. Removal of the film may be monitored optically by observing the color change as a function of time. The appearance of a white color signifies that the Si substrate has been reached. An example of this situation is shown by the optical image in Figure 1. Note that although there are a few pinhole defects, the blue color due to the light interference suggests uniformity, and the white color signifies the region where the Si substrate has been exposed. The local surface roughness, as determined by profilometry measurements is in the range of 5−10 nm. The same order of roughness is observed both on the sugar film and on the etched Si surface. This roughness will ultimately limit the depth resolution of the profiling experiments.

Depth Profiling of Pure Trehalose Films. It is essential to acquire control data so that the behavior of peptide molecules dissolved in the sugar can be compared quantitatively. The response of pure trehalose films to C_{60}^+ ion bombardment is shown in Figure 2. The SIMS signal intensity of the trehalose quasimolecular ion peak at *m*/*z* 325.1, $(M - OH)^+$, and the Si substrate peak at *m*/*z* 28 are plotted versus the C_{60}^+ ion fluence. As shown in the figure, the $(M - OH)^+$ trehalose intensity increases during the initial stages of bombardment, then decreases by a small amount before reaching a steady state level. Finally, the interface between the film and the Si substrate is reached, denoted by the disappearance of the trehalose signal and the appearance of the Si signal. There is a spike in the Si signal at the interface, probably caused by matrix ionization effects associated with the oxidized layer of Si at the Si surface.[32] Another possible explanation is given by the fact that the total sputter yield drops dramatically between the trehalose film and the Si substrate, thus giving rise to an interface maximum caused by a superposition of increasing Si concentration and decreasing sputter yield.

The most important aspect of these data is that the molecular ion signal of trehalose remains stable under continuous C_{60}^+ irradiation. This observation clearly shows that molecule-specific information is being retained. Apparently, fragmented molecules that remain after ion impact are removed by subsequent bombardment events. Similar observations have recently been made during depth profiling of selected polymer, amino acid and Langmuir−Blodgett films under C_{60}^+ and other cluster ion sources.[13,14,18,19] There is also preliminary data illustrating that the molecular ion of diazepam at *m*/*z* 285 doped into human serum albumin retains intensity to doses exceeding 10^{15} ions/cm^2.[33] The case presented here is the first one for which molecular signals greater than *m*/*z* 300 are observed to remain stable indefinitely.

Because of the well-defined nature of these depth profiles, it is feasible to calculate the removal rate and sputtering yield from this material. For this situation, the sputtering yield refers to the number of molecule equivalents of trehalose removed per incident particle, since the calculation is based simply on the amount of material removed. For the film shown in Figure 2, profilometry measurements indicate that the depth of the crater is 800 ± 5 nm. The uncertainty in the measurement arises largely from the intrinsic roughness of the film, as can be discerned for the data shown in the inset of Figure 1. The sputtering yield of molecule equivalents as defined above is determined from the ion fluence and the molecular density as

$$Y = \frac{d \times n}{f} \tag{1}$$

where Y is the sputtering yield in units of molecules per incident ion, d is the measured film thickness, and n represents the molecular density, which is the number of molecules per unit volume. The density of trehalose is 1.54 g/cm^3, therefore n_{tre} is calculated to be 2.7×10^{21} trehalose/cm^3. The fluence of primary ions, f, is expressed in units of ions/cm^2. In our case, the bombardment occurs through the sugar film and into the Si substrate. To estimate the yield of sugar molecules, note that the total amount of material removed is partitioned between the two regions as governed by the relation

$$d = \frac{Y_{tre} f_{tre}}{n_{tre}} + \frac{Y_{Si} f_{Si}}{n_{Si}} \tag{2}$$

where n_{Si} is calculated to be 5×10^{22} Si/cm^3 and where the individual parameters associated with each region are designated by the appropriate subscript. The values of f_{tre} and f_{Si} are obtained by using the sputter time in the film and the substrate, respec-

(32) Ignatova, V. A.; Conard, T.; Moller, W.; Vandervorst, W.; Gijbels, R. *Appl. Surf. Sci.* **2004**, *231−232*, 603−608.
(33) Weibel, D. E.; Lockyer, N.; Vickerman, J. C. *Appl. Surf. Sci.* **2004**, *231−232*, 146−152.

Table 1. Depth Profiling Characteristics of Peptide-doped Trehalose Films

	sample					
	pure trehalose (Tre)	Tre + AGSE	Tre + VGSE	Tre + VGDE	Tre + GGYR	Tre + VGVAPG
MW	342	362	390	418	451	498
film thickness[a] (nm)	330−1090	326−354	314−402	313	350−365	296
sputter time[a] (s)	78−567	33−54	66−246	92.6	279−329	81
field of view[a,b] (μm^2)	400−500	400	400−500	400	450	400
sputter rate[a] (nm/s)	1.4−9.4	7.9−9.9	1.6−4.8	3.38	1.06−1.3	3.65
stage current[a] (nA)	0.25−1	1.2−1.4	0.4−0.8	0.57	0.25−0.32	0.85
sputter rate[a] (nm/nA·s)	4.1−8	5.8−8.6	3.7−6.6	5.9	4.1−4.2	4.3
sputter yield[c] (molecule equivalents/C_{60}^+)	$(4.9 \pm 1.2) \times 10^2$	$(4.8 \pm 1.3) \times 10^2$	$(4.1 \pm 0.3) \times 10^2$	4.0×10^2	$(3.7 \pm 0.2) \times 10^2$	2.8×10^2
interface width (nm)	12.6	19.3	6.2	11.8	12	7.4

[a] The reported range of numbers arises from the variation associated with the fabrication of different films at different times and with variations in the C_{60}^+ ion beam current. [b] The number listed is the side length of a square raster in units of micrometers. [c] Sputtering yield is calculated assuming the density of the film is equal to the density of trehalose (1.54 g/cm^3).

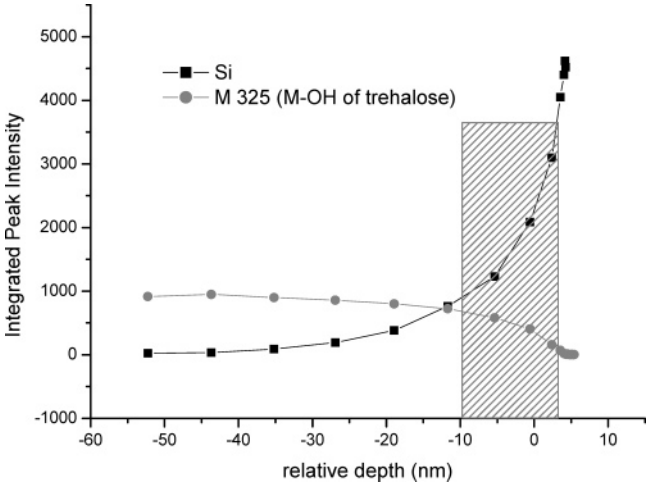

Figure 3. Interface broadening at the trehalose−Si interface. The fluence data shown in Figure 2 are converted to a depth scale using eq 3. The calculated interface width is 12.6 nm from the depth corresponding to 20% and 80% of the maximum Si intensity and is indicated on the figure.

tively, which is determined by the time at which the Si signal reaches 50% of its maximum value.

Using this relation and the dose reported in Figure 2, the sputtering yield of trehalose and the sputtering rate of trehalose and Si can be estimated. Independent measurements suggest a value of ~100 for Y_{si} at 20-keV C_{60}^+ bombardment.[34] Using this value, the trehalose yield computes to 509 molecule equivalents per incident particle for the profile in Figure 2, the sputtering rate is 9.2 nm/s for trehalose, and 0.1 nm/s for Si. The calculated trehalose film thickness is 780 nm, and the Si erosion depth is 20 nm. The parameters necessary to calculate these values are summarized in Table 1. The latter two values are, of course, dependent upon the magnitude of the incident ion beam current density. The high yield and removal rate of trehalose are quite striking. With our source, for example, a 1-μm film may be removed in ~2 min of sputtering. It is interesting that there are 45 atoms in each trehalose molecule, meaning each projectile actually removes about 22 500 atoms!

Another parameter of interest is the apparent width of the interface between the sugar film and the Si substrate. This parameter is important, since it provides a measure of ion-beam-induced mixing effects and, indirectly, the amount of subsurface damage associated with the ion/solid interaction. To estimate the interface width, it is necessary to account for the different sputtering rates associated with the sugar film and the Si substrate. These corrections can be determined by considering the change in sputtering rate using the following relationship[18]

$$\mathrm{SR}_{\mathrm{overall}} = \frac{I_{\mathrm{Si}}}{I_{\mathrm{Si}}^{\mathrm{max}}}\mathrm{SR}_{\mathrm{Si}} + \left(1 - \frac{I_{\mathrm{Si}}}{I_{\mathrm{Si}}^{\mathrm{max}}}\right)\mathrm{SR}_{\mathrm{trehalose}} \qquad (3)$$

where SR is the sputtering rate and I is the integrated peak intensity. With this formula, the primary ion fluence curve may be converted into a depth scale in the region of the interface. A typical example, for which the relative depth scale is plotted with the 0 at the position of the interface, is shown in Figure 3. In this case, the measured interface width is 12.6 nm. This value is clearly influenced by the intrinsic surface roughness of the film of 2−7 nm, as shown in Figure 1. Hence, the interface width due solely to sputtering is on the order of 5−10 nm.

There is currently no theory available to predict these kinds of numbers. Molecular dynamics computer simulations of Ag substrates suggest that the altered layer thickness is ~1.5 nm due to 15-keV C_{60} bombardment.[10,11] Preliminary calculations using an ice matrix suggest that the altered layer thickness is ~8 nm.[35] Our value of 5−10 nm for a trehalose film is consistent with this value.

The intensity of various ions in the mass spectra undergoes changes as the surface of the film is removed. In general, as shown in Figure 4, the quality of the spectrum improves with fluence up to values of 1.5×10^{14} incident ions/cm^2. Several surface impurity peaks are removed, and the chemical noise associated with the spectrum is significantly reduced. In addition to the $(M - OH)^+$ ion at m/z 325, there are three trehalose fragment ions observed at m/z 127, 145, and 163. The proportion of fragment ions to molecular ions increases slightly with ion fluence, as shown in Figure 4, but rapidly reaches a steady value. These data suggest that the nature of the virgin surface and the etched surface are chemically similar and that the properties of the surface rapidly reach a steady state during sputtering.

(34) Hill, R.; Blenkinsopp, P. W. M. *Appl. Surf. Sci.* **2004**, *231−232*, 936−939.

(35) Wojciechowski, I.; Russo, M.; Garrison, B. J. In preparation.

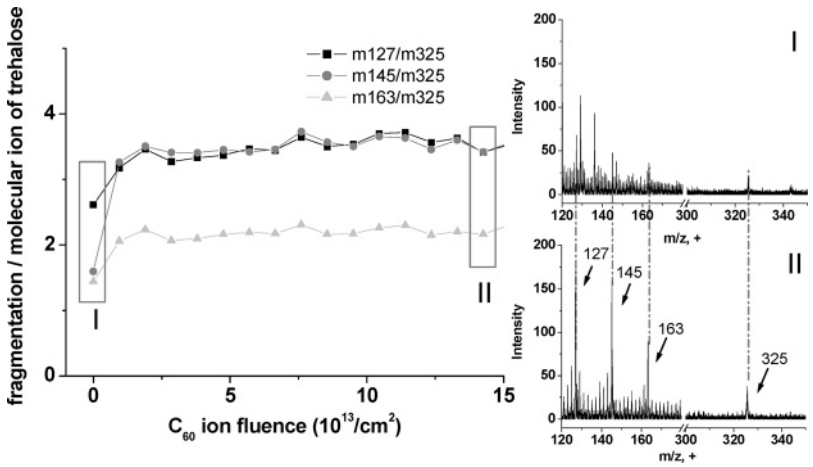

Figure 4. Ratio of the intensity of trehalose fragmentation peaks at *m*/*z* 127, 145, and 163 to trehalose molecular signal at *m*/*z* 325. These ratios are plotted versus the accumulated C_{60}^+ ion fluence. Mass spectra are shown from the region I (surface) and region II (bulk).

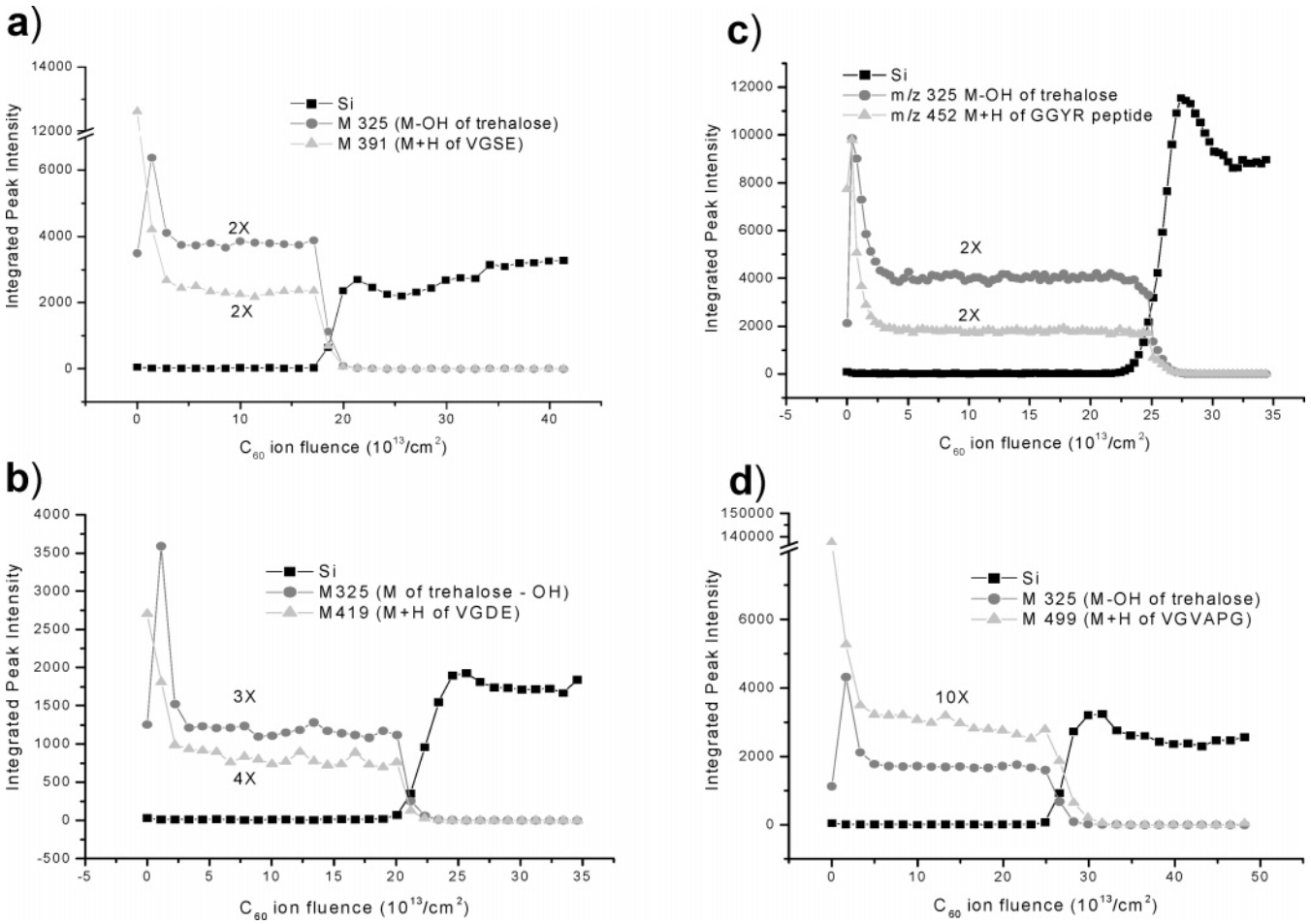

Figure 5. Depth profile of secondary ion intensities versus C_{60}^+ ion fluence of (a) trehalose and VGSE film (318 ± 5 nm), (b) trehalose and VGDE film (315 ± 5 nm), (c) trehalose and GGYR film (352 ± 5 nm), (d) trehalose and VGVAPG film (480 ± 10 nm). Signals are multiplied as indicated on the figure. The VGVAPG film was prepared with a concentration of 1:200 in trehalose, whereas the others were 1:100.

Depth Profiling of Peptide-Doped Trehalose Films. Thin trehalose films doped with peptides may be fabricated in a fashion similar to those described above. Peptide is added to the trehalose solution in a 1:100 molar ratio before spin-coating. Depth profiles for VGSE, VGDE, GGYR, and VGVAPG films prepared using this procedure are shown in Figure 5. These peptides generally exhibit hydrophilic character and do not disrupt the glass formation process that is important for uniform film formation. Hydrophobic peptides with limited water solubility generally do not yield satisfactory films.

In general, the trehalose signal at m/z 325 and the Si signal at m/z 28 exhibit the same behavior reported for the pure films. There is a change of intensity at the surface, followed by a steady state region before the film is removed entirely. The molecular ion intensity of the protein signal is retained throughout the film, although the steady state value is generally 4−50 times lower than

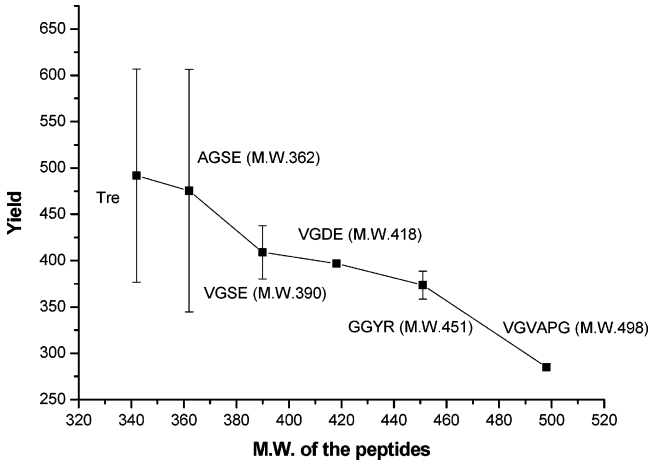

Figure 6. The yield of trehalose molecular equivalents per C_{60} incident ion plotted versus the molecular weight of each peptides. The yield value of the pure trehalose film (Tre) is also included in the plot.

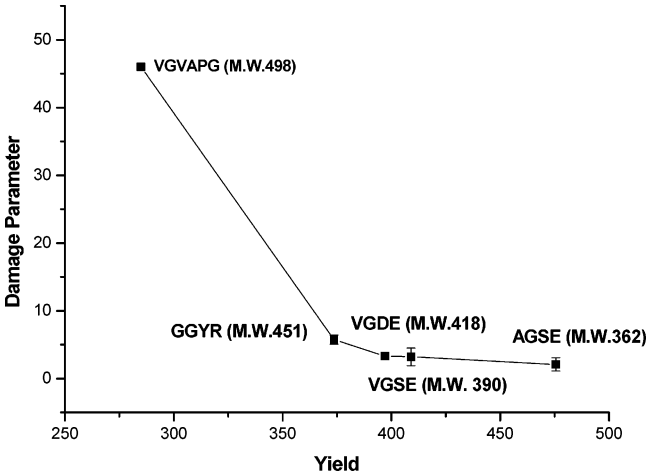

Figure 7. Damage parameter (defined as the ratio of the molecular ion peak intensity in the steady-state region relative to the maximum intensity) versus the sputtering yield of trehalose molecular equivalents. See text for more details about these parameters.

the value found on the virgin surface, depending upon the chemical nature of the specific protein. This level of intensity decrease is acceptable for performing a number of assays under high-dose bombardment conditions.

The observed decrease in the molecular ion intensity may arise from the presence of uncharacterized concentration gradients in the film formed during film preparation, or it could be associated with some accumulated chemical damage inherent in the sputtering process. The first possibility may be assessed at some level by carefully examining the mass spectra as a function of bombardment dose. For example, if the concentration of peptide decreases from the surface to the bulk of the film, the molecular ion signal and the low mass fragment ions should decrease proportionately. As we shall see, these ratios do not behave in this fashion. The factors associated with the second possibility are more difficult to assess. There are no quantitative models to predict when chemical damage becomes important. However, it has been proposed by Gillen and co-workers that damage accumulation is minimized for systems that exhibit a high sputtering yield and a small altered layer thickness.[36]

It is possible to calculate the number of emitted molecules per incident ion and to examine the altered-layer thickness for the peptide-doped films using the same procedure outlined above for the pure trehalose films. These results are summarized in Table 1. The film thicknesses range from 300 to 1000 nm, and the sputtering times required to remove the films range from 30 to 500 s, depending upon the value of the incident ion beam current. The calculated yields of trehalose molecules are found to strongly depend on the nature of the peptide and vary between 290 and 500. These values are larger than those found for metallic systems, but smaller than those reported for ice, for which the yield is observed to be ~2400.[15] The interface widths for all of the peptides films are the same, within experimental error, as those observed for the pure trehalose film.

The results show the interesting trend that the total yield of material decreases with the molecular weight of the incorporated peptide, as shown in Table 1 and Figure 6. Presumably, this decrease is related to the structure of the peptide-doped film. Considering the molar ratio between sugar and peptide of 100:1, each peptide molecule is surrounded by sugar molecules in a tight hydrogen-bonded network. In this environment, it is likely that the peptide stabilizes the sugar film, reducing the sputtering yield of sugar molecules. Larger peptide molecules can bind more trehalose molecules than smaller ones, a result consistent with the observation shown in Figure 6.

It is interesting to speculate about the relationship between the trehalose removal rate and the amount of chemical damage remaining on the surface of the film after ion bombardment. Let us posit that the origin of the decrease in intensity of the peptide molecular ion with dose near the surface is due solely to accumulated damage. If this assumption is correct, then it is possible to estimate the degree of damage by examining the ratio of the maximum molecular ion signal to the steady state value. Hence, large values of this ratio signify extensive chemical damage, and values approaching unity indicate little change in the surface chemistry. The relationship between this damage parameter and the trehalose removal rate is shown in Figure 7. For this limited set of molecules, at least, the predictions of the Gillen model appear to be qualitatively born out: as the yield of trehalose molecules drops below ~300, chemical damage becomes an important mechanism. Above this value, high-quality molecular depth profiling is observed. The mass spectral data associated with the depth profiles suggests that at least part of the decrease in the molecular ion signal with dose arises from chemical damage rather than from any surface segregation of the peptide in the trehalose glass. As shown in Figure 8 for the peptide GGYR, the ratios of various fragment ions to the molecular ion increase with dose, indicating that the surface chemistry is changing slightly due to damage accumulation.

The intensity behavior of other m/z values exhibit interesting changes during the depth profile. Except at the virgin surface, most of the low molecular weight hydrocarbon fragments follow qualitatively the trehalose signal, an expected result, since this species is present in the highest concentration. There are, however, signals associated with residual water of hydration at m/z 18 and 19 that exhibit quite unusual behavior. For GGYR,

(36) Gillen, G.; Simons, D. S.; Williams, P. *Anal. Chem.* **1990**, *62*, 2122−2130.

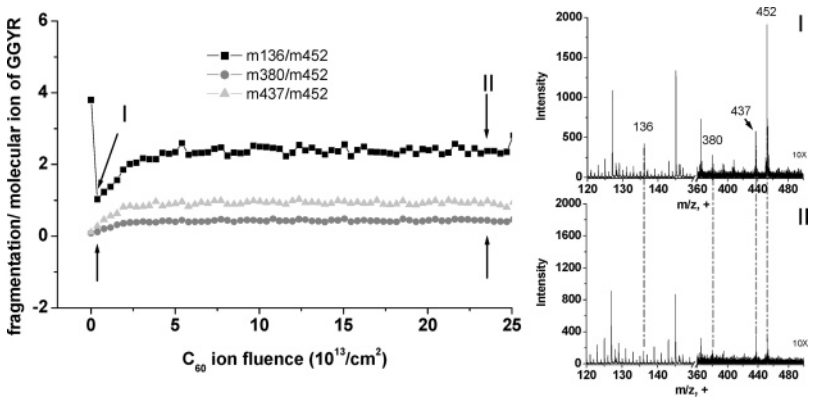

Figure 8. Ratio of the intensity of GGYR fragmentation peaks at *m*/*z* 136, 380, and 437 to the molecular signal of GGYR at *m*/*z* 452 plotted versus the accumulated C_{60}^+ ion fluence. The origin of the fluctuation of the *m*/*z* 136 peak intensity at the surface is unknown. Mass spectra acquired after one sputtering cycle (region I) and after many sputtering cycles (region II) are shown in the inset.

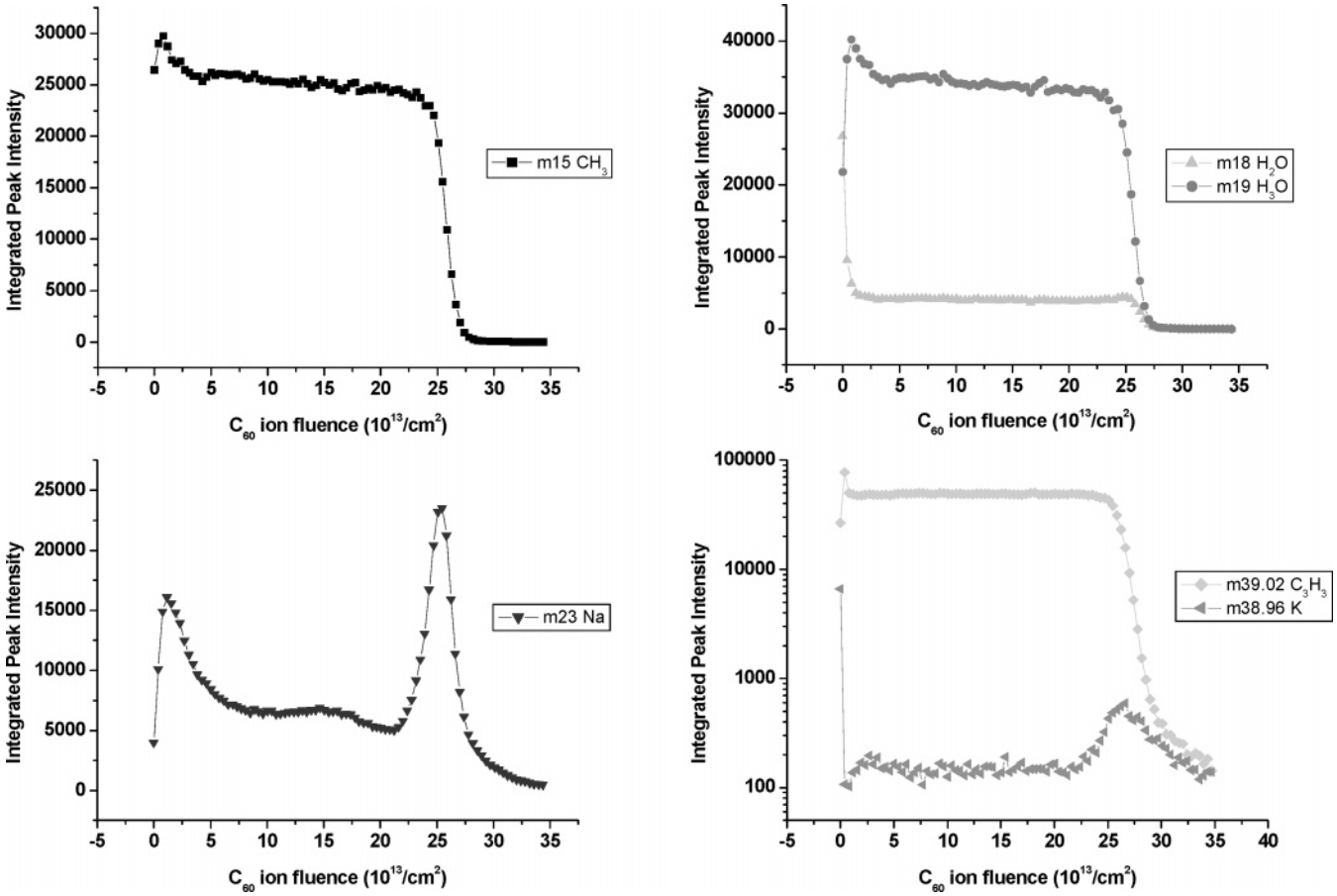

Figure 9. Integrated peak intensities of low-mass peaks, CH_3^+, H_2O^+, H_3O^+, Na^+, K^+, and $C_3H_3^+$ from the GGYR film depth profile plotted versus accumulated C_{60}^+ ion fluence. Note the *m*/*z* 39 profile is plotted on a log scale.

shown in Figure 9, the *m*/*z* 18 intensity rapidly falls to nearly 0 after a dose of only 10^{12} ions/cm^2. The *m*/*z* 19 peak, presumably H_3O^+, increases as a function of dose and then drops slightly into the steady-state region. This increase has also been observed during depth profiling of histamine in an ice matrix,[15] and the reason behind the effect is currently unknown. Finally, alkali ions, such as Na^+ at *m*/*z* 23 and K^+ at *m*/*z* 39, clearly show peak intensities at the interface between the film and the substrate. The *m*/*z* signal of Na^+ also exhibits a maximum intensity near the surface. There is no steady-state region associated with these ions, suggesting that a certain degree of rearrangement occurs either during the bombardment process or during film preparation.

Sample Preparation Issues. Although the sample preparation method described here has provided a platform to prepare high quality films, there are precautions and conditions that require careful attention. For example, films exposed to excessive humidity can lead to crystallization of the glassy state within a matter of hours. Shown in Figure 10 is an optical image along with the associated depth profile of a crystallized film after 12 h of storage at ambient conditions. As expected, the interface is no longer clear, since the crystallized surface exhibits a dramatically

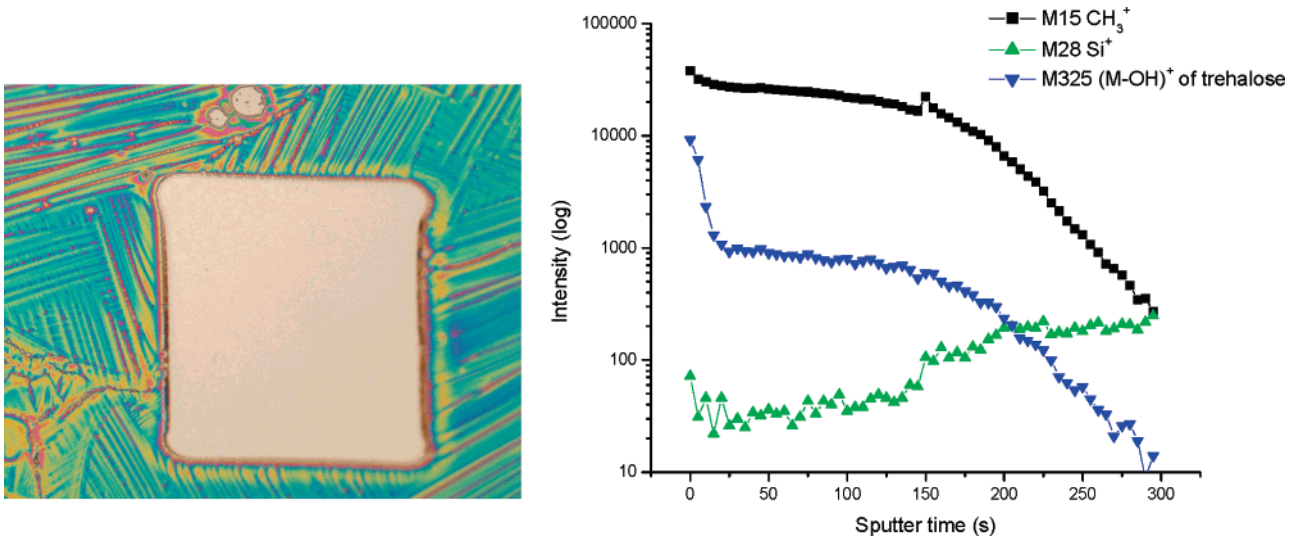

Figure 10. Characteristics of a crystallized film. The depth profile is associated with the optical image shown in the figure. Note that the poor depth resolution due to the high roughness of the crystallized film and the weak Si signal arises because not all of the trehalose has been removed and some of the Si is covered.

rougher surface. The quality of the mass spectra is also dramatically reduced.

CONCLUSION

We have shown that depth profiling of peptide films is possible using glassy trehalose thin films as a matrix and C_{60}^+ projectiles as an erosion source. The results are important not only because they show it is possible to perform such 3-dimensional measurements, but also because the reproducibility of the trehalose platform allows the factors that influence erosion rates, sputtering yields, and damage accumulation effects to be probed in more detail than previously possible. For example, our results support earlier models which assume that a stable molecular ion signal may be retained when the rate of removal of material exceeds the rate of chemical damage. In our case, chemical damage becomes apparent when the number of trehalose molecules removed is less than ~300 per incident C_{60}^+ molecule. With these factors in mind, it should now be feasible to look for other appropriate vehicles which enhance the prospects for depth profiling of molecular solids. Parallel studies in an ice matrix, for example, have also indicated that such measurements are feasible,[15] although the quality of the ice films is not as good as those reported here. In the future, we hope to develop measurement strategies that allow 3-dimensional characterization of various biomaterials, including single biological cells.

ACKNOWLEDGMENT

The authors acknowledge the National Institutes of Health and the National Science Foundation for partial financial support of this work. We also acknowledge Shawn Perry for suggesting the use of the trehalose matrix for these experiments, Dr. Andreas Wucher for his insightful comments, and Professor Xiaoxing Xi for the use of the Dektak profilometer.

Received for review December 17, 2004. Accepted April 4, 2005.

AC048131W